A quaternion-based formulation for the dynamics of tensegrity structures with embedded solid bodies, including structures that are tensionable under load

Thomas Bewley, UC San Diego and NASA Jet Propulsion Laboratory

December 14, 2021

Abstract

This paper is the first in a series of papers that is motivated by the rigging of low-altitude balloon/payload systems with multiple taut ground tethers, analyzed as tensegrity systems. To set the stage for this discussion, in this paper, the statics and dynamics of unconstrained class 1 tensegrity systems with fixed nodes and applied external loads is reviewed and extended as needed for this study. In particular, the classical framework for this class of problems is extended substantially in the present work to account properly for solid bodies embedded within the tensegrity structure. Also, an important distinction is identified between tensegrity designs that are pretensionable, as is classical, and balloon-suspended designs that are only tensionable under load: that is, after the nominal balloon lift and payload weight are applied, there are a few (\bar{n}) remaining degrees of freedom, but these degrees of freedom can only be tuned within a finite range before the balloon itself is effectively pulled down from its desired position. Once the static tension in \bar{n} "control tethers" is set, the resulting tension in the remaining tethers, due to the (known) nominal loads plus the (unknown) disturbance loads, is uniquely determined. A strategy for tuning the static tension in the \bar{n} control tethers is proposed which, in a sense, maximizes the range of unsteady disturbance loads that the tensegrity system can endure before one of the tethers in the system goes slack. The importance of removing any infinitesimal modes from a rigging design is also highlighted.

1 Introduction

As summarized in the abstract, this paper lays the theoretical framework for the static and dynamic analysis of a rigging design (that is, a network of tensile members, a.k.a. strings or tethers, including a number of tethers anchored to various fixed attachment points on the ground) to stabilize a low-altitude balloon/payload system. [Note that, in this (analysis-oriented) paper, we will call the tensile members "strings", as is standard in the literature on tensegrity systems; in our (application-oriented) paper [1], we shift to calling them "tethers", as is standard in the literature on ballooning.] As compared with the use of a single ground tether, as considered in [2, 3], the appropriate use of multiple tethers to secure a (buoyant) balloon and its (heavy) payload to multiple ground attachment points can diminish significantly the deflections in both position and orientation of both the balloon and the payload hanging below it in the presence of variable winds.

Note that, though this analysis was specifically designed to set the stage for the analysis of multiply-tethered balloon/payload systems, the tools developed herein (specifically, for the analysis of tensegrity systems with embedded solid bodies) is quite general, and can be applied to a broad range of other tensegrity systems that are not suspended by balloons, such as the Max Planck CableRobot simulator [4] and related applications.

1.1 Preliminary balloon sizing

In [1], we propose a variety of rigging designs for stabilizing a balloon/payload system at a target payload height H. To set up fair quantitative comparisons of such designs, using both the analysis techniques for the statics and dynamics of tensegrity systems laid out in this paper, as well as corresponding subsequent balloon experiments, all designs considered will restrict the locations of the fixed nodes on the ground to lie within a circle of some radius R; a few representative values of R/H will be considered. We also denote by r the radius of the balloon (assumed in this work to be nearly spherical¹), and by h the vertical distance between the center of the balloon and the center of the payload. We perform some preliminary analysis here to show how to quantify the required balloon size in such

¹Ellipsoidal designs, flattened a bit in the vertical extent, are actually a bit more streamlined in the presence of variable horizontal winds, are found to work a bit better application.

problems; these expressions are calculated for representative applications (hydrogen-filled balloons on Mars, etc.) in [1].

The balloon lift is $L = (\rho_{\rm atm} - \rho_{\rm lift_gas}) g \, 4\pi r^3/3 \propto r^3$. Consider the presence of a horizontal wind of maximum speed w, and identify the balloon Reynolds number $Re = 2rw/\nu_{atm}$. The drag of the balloon in the presence of this wind is $D = C_d \, \rho_{\rm atm} \, \pi r^2 \, w^2/2 \propto r^2 w^2$, where $C_d \approx 0.2$ for $Re \gtrsim 10^6$ (that is, in the post-critical separated flow regime with a turbulent boundary layer over a smooth balloon surface). Define also the excess lift, $E = L - W_{\rm hull} - W_{\rm tethers} - W_{\rm payload}$, as the lift L of the balloon minus the weight of the fabric forming the balloon surface, $W_{\rm hull} = \rho_{\rm hull} \, 4\pi r^2$, the weight of the rigging, $W_{\rm tethers} \approx p \, \rho_{\rm tethers} \sqrt{R^2 + H^2}$ (where p is the number of ground tethers used), and the (given) weight of the payload, $W_{\rm payload}$.

To simplify the initial analysis, consider first a 2D setting in which r and h are small compared to R and H. In this case, the two outer tethers between the balloon and the ground (see, e.g., Figure 1) form essentially an isosceles triangle, with the angle γ at its top vertex satisfying $\gamma/2 \approx \operatorname{atan}(R/H)$. Analyzing the force vector at this vertex, it is plainly evident that both tethers in this setting will stay in tension, with the upwind tether carrying progressively higher tension compared to the downwind tether as the wind speed w is increased, until the ratio D/E of the horizontal to (total) vertical forces at this vertex reach the proportion R/H; that is, to keep the downwind tether from going slack, we require that

$$\frac{R}{H} \ge \frac{D}{E} \approx \frac{C_d \,\rho_{\text{atm}} \,\pi r^2 \,w^2/2}{\left(\rho_{\text{atm}} - \rho_{\text{lift_gas}}\right) g \,4\pi r^3/3 - \rho_{\text{hull}} \,4\pi r^2 - p \,\rho_{\text{tethers}} \sqrt{R^2 + H^2} - W_{\text{payload}}}.$$
(1)

Note that, for a given maximum wind speed w, the drag-to-lift ratio $D/L \propto 1/r$ is reduced as r is increased. For r that is too small, the balloon lift is barely sufficient to hoist the payload, the denominator on the RHS of (1) is small, and a very large R is required for a given H. Increasing r, the lift term in the denominator on the RHS grows faster than both the numerator and the other terms in the denominator, and equality in (1) is eventually reached. For a given target H, an intermediate R/H is generally necessary, as large R/H require long tethers, which risk sagging and fouling, and a small R/H require a larger balloon radius r, by (1). Once the geometric factor R/H is chosen for a given payload weight $W_{\rm payload}$, a given payload height H, a specified maximum horizontal wind speed w, and various material and gas properties, an appropriate minimum balloon radius r may be selected simply by solving (1) [numerically] for r.

For 3D implementations, the p points on the ground form a regular polygon of circumradius R. For p=3, these points form an equilateral triangle with inradius $R_{\rm in}=R/2$, whereas for p=4 they form a square with inradius $R_{\rm in}=R/\sqrt{2}$. In the 3D case, the minimum balloon size r may be selected via (1) as discussed previously in the 2D case if the prevailing wind direction is well known (so that a tether may be oriented in the upwind direction); if the prevailing wind direction is not well known, however, the worst case may be considered by taking the upwind direction as halfway between the tether directions, and the formula given in (1) should thus replace R with $R_{\rm in}$; it is seen in this setting that fourfold symmetry pays a significantly lower penalty than threefold symmetry $(1/\sqrt{2} \text{ rather than } 1/2)$.

1.2 Two initial 2D rigging designs

To highlight the precise notation used in this discussion, and to illustrate the essential issue of infinitesimal modes, two initial 2D rigging designs (Design W, which is "wobbly", and Design S, which is "stable") are provided in Figure 1. These initial 2D rigging designs are provided for illustration purposes only; any practical balloon rigging design, of course, must be 3D. Since the design of practical 3D rigging configurations involves a rather complex set of application-specific tradeoffs, our introductory discussion of the tradeoffs involved in the full 3D rigging design problem is deferred to [1], allowing us to focus on the associated tensegrity analysis framework here.

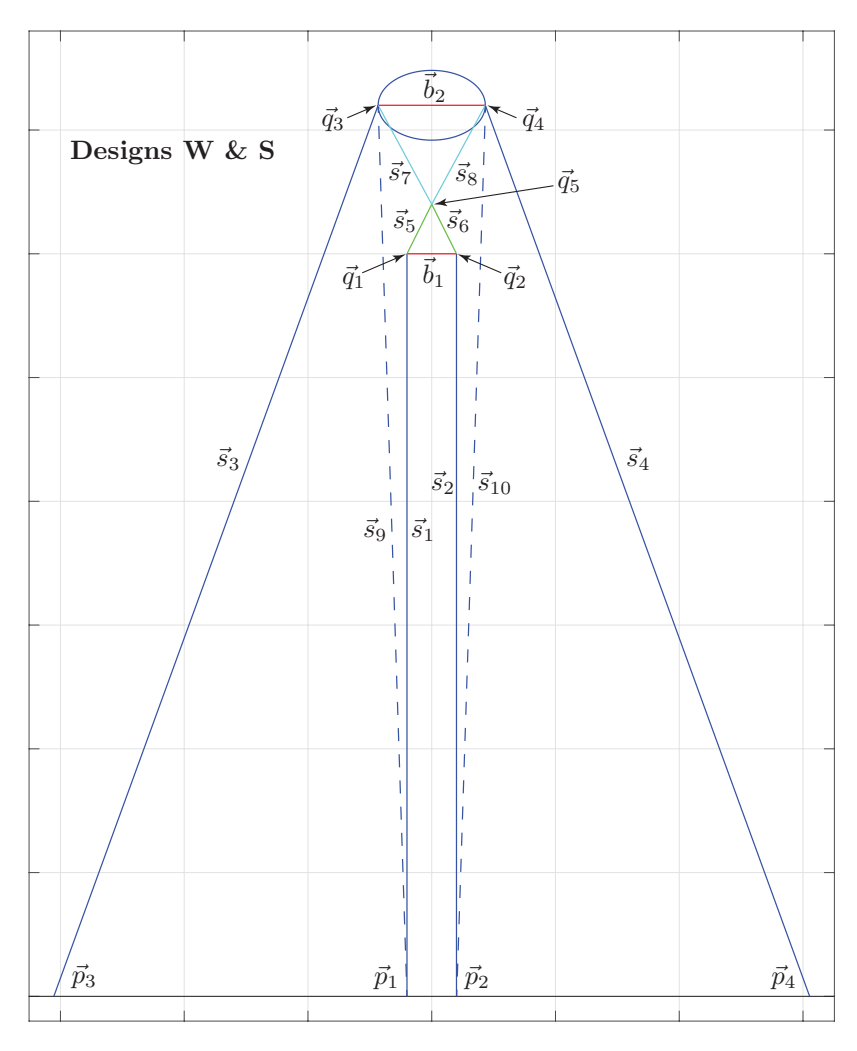


Figure 1: 2D balloon rigging designs W (without tethers s_9 and s_{10}) and S (including tethers s_9 and s_{10}), indicating the notation used in the present analysis. The (heavy) payload is represented as bar \vec{b}_1 , with (effectively, massless) strings (a.k.a. tethers) \vec{s}_1 and \vec{s}_2 , attached at free nodes \vec{q}_1 and \vec{q}_2 (at the ends of this bar) connecting to ground points \vec{p}_1 and \vec{p}_2 . The (buoyant) balloon is represented as bar \vec{b}_2 , with strings \vec{s}_3 and \vec{s}_4 attached at the free nodes \vec{q}_3 and \vec{q}_4 and connecting to ground points \vec{p}_3 and \vec{p}_4 . The convergence point \vec{q}_5 , another free node, is attached to the nodal points on the payload, \vec{q}_1 and \vec{q}_2 , via tethers \vec{s}_5 and \vec{s}_6 . The convergence point \vec{q}_5 is also attached to the nodal points on the balloon, \vec{q}_3 and \vec{q}_4 , via a single tether, \vec{s}_7 - \vec{s}_8 , routed through a pulley at \vec{q}_5 , thereby equalizing the tension on these two strings and effectively isolating the pitching of the balloon \vec{b}_2 from the orientation of the payload \vec{b}_1 (thus, the balloon essentially just supplies a "lift" force to the payload). As shown in the text, the addition of s_9 and s_{10} , connecting the balloon nodal points \vec{q}_3 and \vec{q}_4 to the ground points \vec{p}_1 and \vec{p}_2 , respectively, removes the "infinitesimal" modes otherwise associated with the structure, thereby converting from a \underline{W} obbly rigging design to a Stable rigging design. Note that the considerations embodied in these initial 2D "cartoons" are extended to practical 3D rigging designs in [1].

2 Static equilibrium of tensegrity structures

2.1 Free nodes, fixed nodes, bars, and strings

Following closely the analysis of the static equilibrium of tensegrity structures in chapter 2 of [10], augmenting its notation slightly as necessary (see, e.g., Figure 1), consider a 2D or 3D structure with:

- q free nodes $\{\vec{q}_1,\ldots,\vec{q}_q\}$ and p fixed nodes $\{\vec{p}_1,\ldots,\vec{p}_p\}$, collectively called the n=q+p nodes $\{\vec{n}_1,\ldots,\vec{n}_n\}$, and
- $b \ \underline{b} ars \ \{\vec{b}_1, \dots, \vec{b}_b\}$ and $s \ \underline{s} trings \ \{\vec{s}_1, \dots, \vec{s}_s\}$, collectively called the $m = b + s \ \underline{m} embers \ \{\vec{m}_1, \dots, \vec{m}_m\}$.

For the purpose of analyzing static equilibria in §2, solid bodies with n attachment points may be modelled simply as clusters of n(n-1)/2 interconnected bars (i.e., with one bar between each two points on the body); as an example, for the purpose of static equilibrium analysis of the 2D structures indicated in Figure 1, both the balloon and the payload are modelled as single bars $(\vec{b}_1 \text{ and } \vec{b}_2)$. This crude model is substantially refined in order to account properly for solid-body dynamics in §3. The nodal locations \vec{n}_i are each vectors from the origin in \mathbb{R}^d , where d=2 or 3 is the dimension of the problem considered, and are denoted as follows²:

$$Q = \begin{bmatrix} \vec{q}_1 & \cdots & \vec{q}_q \end{bmatrix}, \quad \mathbf{q} = \text{vec}(Q) = \begin{bmatrix} \vec{q}_1 \\ \vdots \\ \vec{q}_q \end{bmatrix}, \quad P = \begin{bmatrix} \vec{p}_1 & \cdots & \vec{p}_p \end{bmatrix}, \quad \mathbf{p} = \text{vec}(P) = \begin{bmatrix} \vec{p}_1 \\ \vdots \\ \vec{p}_n \end{bmatrix}$$

$$\Rightarrow \quad \begin{bmatrix} Q & P \end{bmatrix} = N = \begin{bmatrix} \vec{n}_1 & \cdots & \vec{n}_n \end{bmatrix}, \quad \mathbf{n} = \begin{bmatrix} \mathbf{q} \\ \mathbf{p} \end{bmatrix} = \text{vec}(\begin{bmatrix} Q & P \end{bmatrix});$$
(2a)

 \mathbf{q} and Q, which define the locations of the free nodes, are sometimes called the *configuration vector* and *configuration matrix*, respectively, of the tensegrity structure. Each member $\vec{m}_k = \vec{n}_{k,1} - \vec{n}_{k,2}$ connects two nodes, $\vec{n}_{k,1}$ and $\vec{n}_{k,2}$, at least one of which is free (e.g., in Figure 1, $\vec{m}_1 = \vec{b}_1 = \vec{n}_2 - \vec{n}_1 = \vec{q}_2 - \vec{q}_1$), and are denoted as follows:

$$B = \begin{bmatrix} \vec{b}_1 & \cdots & \vec{b}_b \end{bmatrix}, \quad \mathbf{b} = \text{vec}(B) = \begin{bmatrix} \vec{b}_1 \\ \vdots \\ \vec{b}_b \end{bmatrix}, \quad S = \begin{bmatrix} \vec{s}_1 & \cdots & \vec{s}_s \end{bmatrix}, \quad \mathbf{s} = \text{vec}(S) = \begin{bmatrix} \vec{s}_1 \\ \vdots \\ \vec{s}_s \end{bmatrix}$$

$$\Rightarrow \quad \begin{bmatrix} B & S \end{bmatrix} = M = \begin{bmatrix} \vec{m}_1 & \cdots & \vec{m}_m \end{bmatrix}, \quad \mathbf{m} = \begin{bmatrix} \mathbf{b} \\ \mathbf{s} \end{bmatrix} = \text{vec}(\begin{bmatrix} B & S \end{bmatrix}).$$
(2b)

It is also useful to define a vector of member lengths ℓ , including a vector of bar lengths ℓ^b and a vector of string lengths ℓ^s , as well as a vector of normalized member directions \mathbf{d} , including a vector of normalized bar directions \mathbf{d}^b and a vector of normalized string directions \mathbf{d}^s , such that

$$\ell_{k} = \|\vec{m}_{k}\|, \qquad \ell_{i}^{b} = \|\vec{b}_{i}\|, \qquad \ell_{j}^{s} = \|\vec{s}_{j}\|, \qquad \ell = \begin{bmatrix} \boldsymbol{\ell}^{b} \\ \boldsymbol{\ell}^{s} \end{bmatrix},$$

$$\vec{d}_{k} = \vec{m}_{k}/\ell_{k}, \qquad \vec{d}_{i}^{b} = \vec{b}_{i}/\ell_{i}^{b}, \qquad \vec{d}_{j}^{s} = \vec{s}_{j}/\ell_{j}^{s}, \qquad \mathbf{d} = \begin{bmatrix} \mathbf{d}^{b} \\ \mathbf{d}^{s} \end{bmatrix} = \text{vec}(D),$$

$$D = \begin{bmatrix} \vec{d}_{1} & \cdots & \vec{d}_{m} \end{bmatrix} = \begin{bmatrix} D^{b} & D^{s} \end{bmatrix}, \quad D^{b} = \begin{bmatrix} \vec{d}_{1}^{b} & \cdots & \vec{d}_{b}^{b} \end{bmatrix}, \quad D^{s} = \begin{bmatrix} \vec{d}_{1}^{s} & \cdots & \vec{d}_{s}^{s} \end{bmatrix};$$

$$(2c)$$

note that $\|\vec{d}_k(t)\| = 1$ for all t. Following [10], the connectivity of a structure, relating the n nodes N in (2a) to the m members M in (2b), is described easily via its <u>connectivity matrix</u> C, defined and partitioned such that

$$M = N C^T$$
, $C = \begin{bmatrix} C_Q & C_P \end{bmatrix} = \begin{bmatrix} C_B \\ C_S \end{bmatrix} \Rightarrow \begin{bmatrix} B & S \end{bmatrix} = \begin{bmatrix} Q & P \end{bmatrix} \begin{bmatrix} C_Q^T \\ C_P^T \end{bmatrix} = \begin{bmatrix} Q & P \end{bmatrix} \begin{bmatrix} C_B^T & C_S^T \end{bmatrix}$, (2d)

where, denoting \mathbf{e}_j as the vector in the j'th column of the identity matrix, each column of C^T is given by $(\mathbf{e}_{k,1} - \mathbf{e}_{k,2})$, indicating the two nodes $\vec{n}_{k,1}$ and $\vec{n}_{k,2}$ that member \vec{m}_k connects, with one entry equal to 1, one entry equal to -1, and all other entries equal to zero. For the illustrative example structures shown in Figure 1, the first column of C^T is $\begin{pmatrix} -1 & 1 & 0 & \dots & 0 \end{pmatrix}^T$, indicating that the bar \vec{b}_1 connects free nodes \vec{q}_1 and \vec{q}_2 .

²All vectors in \mathbb{R}^d are denoted with an arrow (e.g., \vec{q}_i). All other vectors, and quaternions, are denoted in bold (e.g., \mathbf{q}).

2.2Forces

Consider also external forces $\{\vec{u}_1,\ldots,\vec{u}_q\}$, including the effects of the weight or buoyancy of the bars themselves³. applied to each of the q free nodes, and reaction forces $\{\vec{v}_1,\ldots,\vec{v}_p\}$ at each of the p fixed nodes, and similarly denote

$$U = \begin{bmatrix} \vec{u}_1 & \cdots & \vec{u}_q \end{bmatrix}, \quad \mathbf{u} = \text{vec}(U), \quad V = \begin{bmatrix} \vec{v}_1 & \cdots & \vec{v}_p \end{bmatrix}, \quad \mathbf{v} = \text{vec}(V), \quad W = \begin{bmatrix} U & V \end{bmatrix}.$$

Internally, denote⁴ by $(\vec{d}_k x_k)$ and $-(\vec{d}_k x_k)$ the forces that member \vec{m}_k applies at nodes $\vec{n}_{k,2}$ and $\vec{n}_{k,1}$, respectively, where x_k denotes the tension force (if positive) or compression force (if negative) in member \vec{m}_k . Thus, the internal member forces may be written

$$DX = \begin{bmatrix} D^{b} & D^{s} \end{bmatrix} \begin{bmatrix} X^{b} & 0 \\ 0 & X^{s} \end{bmatrix} = \begin{bmatrix} D^{b} X^{b} & D^{s} X^{s} \end{bmatrix},$$
where $X = \operatorname{diag}(\mathbf{x}), \quad \mathbf{x} = \begin{bmatrix} \mathbf{x}^{b} \\ \mathbf{x}^{s} \end{bmatrix}, \quad X^{b} = \operatorname{diag}(\mathbf{x}^{b}), \quad X^{s} = \operatorname{diag}(\mathbf{x}^{s}).$

$$(3a)$$

It is assumed that bars can carry compressive or tensile forces, but strings can only carry tensile forces, and thus $x_i^s \geq 0$ for $j=1,\ldots,s$. Following [10], the cumulative force f_k at each node \vec{n}_k , due to the sum of all of the internal forces applied by each connected member \vec{m}_i (that is, due to the compression and tension forces of all the bars and strings), is then given simply by applying the connectivity matrix C to the above expression such that

$$\begin{bmatrix} \vec{f}_1 & \cdots & \vec{f}_n \end{bmatrix} = F = -DXC, \tag{3b}$$

with the minus sign because positive x_k denotes tension forces in the member direction d_k . Static equilibrium is reached when sum of the internal forces at each node, F, is in balance with (that is, equal and opposite to) the external forces W at each node such that

$$F = -DXC = -W \Rightarrow DXC = \begin{bmatrix} U & V \end{bmatrix}.$$

For any tensegrity structure with b bars B and s strings S connecting q free nodes Q and p fixed nodes P via the connectivity matrix C, as related in (2d), with external forces U applied at each free node, static equilibrium thus gives a linear system of equations in the m unknown forces $\{x_1,\ldots,x_m\}$ and the p unknown reaction forces V. As discussed further in $\S 2.4$, this linear system of equations may have 0, 1, or ∞ solutions, depending on the setup of the problem. The problem of determining the static equilibrium may be simplified by leveraging the partitioning $C = |C_Q - C_P|$, and first solving for the forces at static equilibrium via

$$DXC_{Q} = U. (4a)$$

These conditions of static equilibrium, which are linear in the unknown member forces x_k , may easily be rewritten in terms of the vector \mathbf{x} in the standard matrix/vector form

$$A_{\rm se}\mathbf{x} = \mathbf{u} \tag{4b}$$

by applying the identities

$$\operatorname{vec}(DXC_Q) = (C_Q^T \otimes D)\operatorname{vec}(X), \quad \operatorname{vec}(X) = \operatorname{vec}(\operatorname{diag}(\mathbf{x})) = A_{\mathbf{fe}}\mathbf{x},$$

where

- $\operatorname{vec}(\cdot)$ denotes the standard vectorization operation that converts a matrix to a vector,
- \otimes denotes the standard Kronecker product,
- e^i , for i = 1, ..., n, denotes the canonical basis vectors of \Re^n ,
- \mathbf{f}^j , for $j=1,\ldots,n^2$, denotes the canonical basis vectors of \Re^{n^2} , and the $n^2 \times n$ matrix $A_{\mathbf{fe}} = \sum_{i=1}^n \mathbf{f}^{n(i-1)+i} \otimes (\mathbf{e}^i)^T$,

from which it follows immediately that

$$A_{\rm se} = (C_Q^T \otimes D) A_{\rm fe}. \tag{4c}$$

Equation (4b) may be solved, after which the reaction forces $\mathbf{v} = \text{vec}(V)$ may be computed directly via $V = DXC_P$.

$$DX = M\Sigma = \begin{bmatrix} B & S \end{bmatrix} \begin{bmatrix} -\Lambda & 0 \\ 0 & \Gamma \end{bmatrix} = \begin{bmatrix} -B\Lambda & S\Gamma \end{bmatrix} \quad \text{where} \quad \Sigma = \operatorname{diag}(\sigma_1, \dots, \sigma_m), \quad \Lambda = \operatorname{diag}(\lambda_1, \dots, \lambda_b), \quad \Gamma = \operatorname{diag}(\gamma_1, \dots, \gamma_s).$$

³Note: with this approach, this effect must be lumped, in an approximate fashion, at each free node associated with each solid body. ⁴Note that [10] defines and solves for the force density $\sigma_k = x_k/\ell_k$ in each member, rather than solving for the forces x_k themselves (where, again positive σ_k denotes tension and negative σ_k denotes compression). They further denote the force density in string \vec{s}_j by γ_i (with, again, $\gamma_i > 0$ denoting tension), and the force density in bar \bar{b}_i by λ_i (with, in contrast, $\lambda_i > 0$ denoting compression). Using that (slightly more complicated) notation, the present derivation is expressed by applying the relations

Brief review of the Singular Value Decomposition (SVD)

Consider for a moment an arbitrary $\hat{m} \times \hat{n}$ matrix \hat{A} . It will be useful in the three subsections that follow to refer to the components of the block decomposition of the SVD, which may be defined as follows:

$$\hat{A}_{\hat{m}\times\hat{n}} = U_{\hat{m}\times\hat{m}} \Sigma_{\hat{m}\times\hat{n}} V_{\hat{n}\times\hat{n}}^H = \begin{bmatrix} \underline{U}_{\hat{m}\times\hat{r}} & \overline{U}_{\hat{m}\times(\hat{m}-\hat{r})} \end{bmatrix} \begin{bmatrix} \underline{\Sigma}_{\hat{r}\times\hat{r}} & 0 \\ 0 & 0 \end{bmatrix} \begin{bmatrix} \underline{V}_{\hat{n}\times\hat{r}} & \overline{V}_{\hat{n}\times(\hat{n}-\hat{r})} \end{bmatrix}^H,$$

where Σ is diagonal with real, non-negative elements σ_i on the main diagonal, arranged in descending order, U and V are unitary, and \hat{r} is the rank of the matrix \hat{A} . Note that $\hat{A} = U\Sigma V$. Much can be said about the matrix \hat{A} based on this decomposition. For the present purposes, recall simply that, for any $\hat{m} \times \hat{n}$ matrix \hat{A} ,

- (i) \hat{r} is both the number of independent rows of \hat{A} and the number of independent columns of \hat{A} ,
- (ii) the columns of \hat{A} are spanned by the \hat{r} orthogonal columns of U,
- (iii) the rows of \hat{A} are spanned by the \hat{r} orthogonal rows of V^H ,
- (iv) the nullspace of \hat{A} (all **x** such that \hat{A} **x** = 0) is spanned by the $\hat{n} \hat{r}$ orthogonal columns of \overline{V} ,
- (v) the left nullspace of \hat{A} (all \mathbf{y} such that $\hat{A}^H \mathbf{y} = 0$) is spanned by the $\hat{m} \hat{r}$ orthogonal columns of \overline{U} , (vi) using the *Moore-Penrose pseudoinverse* $\hat{A}^+ = \underline{V}\underline{\Sigma}^{-1}\underline{U}^H$, the least-squares solution to $\hat{A}\mathbf{x} = \mathbf{b} + \boldsymbol{\epsilon}$, minimizing the norm of both ϵ and \mathbf{x} , is $\mathbf{x} = \hat{A}^{\dagger} \mathbf{b}$,
 - (vii) for full-rank tall matrices, $\hat{r} = \hat{n} < \hat{m}$, and $\hat{A}^+ = (\hat{A}^T \hat{A})^{-1} \hat{A}^T$ is the unique left inverse such that $\hat{A}^+ \hat{A} = I$, (viii) for full-rank fat matrices, $\hat{r} = \hat{m} < \hat{n}$, and $\hat{A}^+ = \hat{A}^T (\hat{A} \hat{A}^T)^{-1}$ is the unique right inverse such that $\hat{A}\hat{A}^+ = I$,

 - (ix) for nonsingular square matrices, $\hat{r} = \hat{m} = \hat{n}$, and $\hat{A}^+ = \hat{A}^{-1}$ is the unique inverse of \hat{A} .

2.4 SVD analysis of the conditions of static equilibrium

The linear system of equations (4b) governing the member forces \mathbf{x} at static equilibrium of a proposed tensegrity structure may have 0, 1, or an infinite number of solutions. Stated differently, performing an SVD of the $\hat{m} \times \hat{n}$ matrix A_{se} , with $\hat{m} = dq$ and $\hat{n} = b + s$ (where d is the dimension of the problem considered, q is the number of free nodes, b is the number of bars, and s is the number of strings), the problem in (4b) is said to be:

- (a) potentially inconsistent if $\hat{r} < \hat{m}$, and thus $A_{\rm se}$ has some rows which are linearly dependent on the other rows in this case, (4b) will either have 0 solutions or at least one solution, depending upon whether or not the external force vector **u** is spanned by the columns of U, and/or
- (b) underdetermined if $\hat{r} < \hat{n}$, and thus there are fewer independent equations than there are unknowns [in this case, if (4b) has one solution **x**, then **x** plus any linear combination of the $\overline{n} = \hat{n} - \hat{r}$ columns of \overline{V} is also a solution]. The equations of static equilibrium (4b) may thus be:
 - potentially inconsistent only $(\hat{m} > \hat{r} = \hat{n})$, with 0 or 1 solution depending on **u**,
 - underdetermined only $(\hat{n} > \hat{r} = \hat{m})$, with ∞ solutions,
 - both potentially inconsistent and underdetermined $(\hat{n} > \hat{r}, \hat{m} > \hat{r})$, with 0 or ∞ solutions depending on **u**, or
- neither potentially inconsistent nor underdetermined $(\hat{n} = \hat{m} = \hat{r})$, with exactly 1 solution (this condition is called *static determinance*).

A tensegrity structure together with a nominal loading profile \mathbf{u}_0 will be called realizable if at least one solution to (4b) exists with all strings in tension for this nominal loading profile; note in particular that, even if (4b) is statically determinant, the corresponding tensegrity structure may not be realizable for this nominal loading profile if the corresponding force distribution \mathbf{x} does not have all strings in tension.

2.5Infinitesimal mechanisms in potentially inconsistent tensegrity structures

If $A_{\rm se}$ is potentially inconsistent, with $\hat{r} < dq$, then a corresponding tensegrity configuration with a realizable equilibrium for the nominal loading \mathbf{u}_0 has infinitesimal mechanisms associated with zero deformation energy. Such a configuration can be either unstable or soft. The first case (instability) is, clearly, catastrophic, with small disturbances acting on the structure leading rapidly to failure—visualize two opposing bars, under compression, meeting at a node (i.e., a ball joint) where external disturbance forces may be applied, with no strings attached to stabilize.

The second case (soft or "wobbly" modes), though not catastrophic, is also a highly undesirable feature for a tensegrity structure—visualize two opposing strings, under tension, meeting at a node where external forces may be applied. In this case, assuming all bars are rigid and strings non-stretchable, there are no finite force densities in the members that can sustain a range of disturbances on the nodes (specifically, any disturbances u generated with components in the directions of the columns of \overline{U}) for this free node configuration q. However, assuming (much more realistically) that the strings are somewhat *elastic* (and, again, that the system is realizable for the nominal loading), a significant deformation of the free node configuration vector \mathbf{q} (computed using the techniques of §3) may well lead to a deformed configuration that can sustain the problematic disturbance profile. Unfortunately, a different disturbance profile will generally lead to a different deformation of the structure, so this approach generally leads to a rather "wobbly" structure in the presence of unsteady external loads. Soft modes are thus also generally undesirable in a tensegrity structure, as they easily lead to relatively large deflections in response to small disturbances.

Fortunately, as discussed further in [7], the condition of potential inconsistency in (4b), with r < dq (and, the corresponding presence of unstable or soft modes), can usually be removed entirely from a tensegrity structure with a given configuration of bars simply by judiciously adding more strings, thereby increasing r if the new strings are well positioned (see, e.g., strings \vec{s}_9 and \vec{s}_{10} in Figure 1).

2.6 Static tensioning of an (underdetermined) pretensionable tensegrity structure

If $A_{\rm se}$ is underdetermined, with r < b + s, then there are fewer independent equations than unknowns in (4b). This situation generally admits a certain control authority over the force distribution in the members, which can be useful if leveraged correctly. It is noted that most structures considered in the framework of tensegrity systems are, in fact, underdetermined. Further, most underdetermined tensegrity systems considered in the existing literature, with the notable exception of those proposed here, are pretensionable, with a range of realizable force density distributions in the members (that is, with all strings in tension) possible even for zero nominal loading, $\mathbf{u}_0 = 0$. [The special case of underdetermined tensegrity structures that are not pretensionable, but still tensionable under load (meaning that there is a range of realizable force density distributions in the members, with all strings in tension, for some nonzero nominal external load, $\mathbf{u}_0 \neq 0$), is discussed further in §2.7.]

In the pretensionable setting, the question remains of how to adjust the remaining degrees of freedom in the structure such that all strings remain taut as time-varying nominal loads plus disturbances, $\mathbf{u}(t)$, are applied to the system, with the tensions greater than or equal to some minimum level $\tau_{\min} > 0$ in all strings to assure that none go slack, while the tensions in all strings in the structure also do not get too large, thereby risking failure. One convenient approach to address this problem is by framing it as a simple Linear Program (LP), as discussed below. [This approach is modified slightly in §2.7 for the case of underdetermined tensegrity structures that are not pretensionable, but are still tensionable under load.]

We start by assuming (that is, idealizing) that the strings are nonstretchable, and rewrite the equations of static equilibrium of a pretensionable tensegrity structure, $A_{se}\mathbf{x} = \mathbf{u}$, as

$$A_{\rm se}(\mathbf{x} + \boldsymbol{\delta}) = \mathbf{u}.$$

If $A_{\rm se}$ is underdetermined and the strings are idealized as nonstretchable, the distribution of (compression and tension) forces in the members, \mathbf{x} , may be replaced by $(\mathbf{x} + \boldsymbol{\delta})$ at any instant, where $\boldsymbol{\delta} = \overline{V}\mathbf{c}$ is any linear combination of the columns of \overline{V} (the vectors in the nullspace of $A_{\rm se}$), without affecting the static equilibrium itself. Assume we are starting from some static equilibrium condition $A_{\rm se}\mathbf{x} = \mathbf{u}$ for some (unknown) external loading $\mathbf{u}(t)$, and denote $\widetilde{\mathbf{x}}$ as the subset of the tensions in the \widetilde{m} measurable strings (i.e., those for which we can actually measure their tension⁵), $\widetilde{\boldsymbol{\delta}}$ as the corresponding elements of $\boldsymbol{\delta}$, and \widetilde{V} as the corresponding rows of \overline{V} . To assure, with some margin for error, that none of these \widetilde{m} strings go slack while not disrupting the static equilibrium achieved by the structure, we seek at any given timestep to update \mathbf{x} with $\boldsymbol{\delta}$ while respecting the \widetilde{m} conditions (written here in vector form) that

$$\widetilde{\mathbf{x}} + \widetilde{\boldsymbol{\delta}} \ge \tau_{\min} \mathbf{1}$$
 where $\widetilde{\boldsymbol{\delta}} = \widetilde{\overline{V}} \mathbf{c} \implies -\widetilde{\overline{V}} \mathbf{c} \le \widetilde{\mathbf{x}} - \tau_{\min} \mathbf{1}$ (5a)

for some (pre-selected) positive minimum tension τ_{\min} , where **1** is a vector with each element unity, and a vector inequality $\mathbf{a} \leq \mathbf{b}$ denotes element-wise inequality, $a_i \leq b_i$ for all i. We generally want to select the coefficient vector \mathbf{c} to achieve (5a) without letting any of the \widetilde{m} measurable tensions get too large. One convenient way of achieving this is to minimize a weighted one-norm of the value of $\widetilde{\mathbf{x}}$ after it is incremented by $\widetilde{\boldsymbol{\delta}}$; i.e., assuming \mathbf{x} is realizable (with no slack strings, so that $\widetilde{x}_m > 0$ for all of the \widetilde{m} measurable strings, and thus $C_0 = \mathbf{w}^T \widetilde{\mathbf{x}} > 0$), to solve

$$\underset{\mathbf{c}}{\operatorname{argmin}} \mathbf{w}^{T} (\widetilde{\mathbf{x}} + \widetilde{\overline{V}} \mathbf{c}) = C_{0} - \underset{\mathbf{c}}{\operatorname{argmax}} \widetilde{\mathbf{w}}^{T} \mathbf{c} \quad \text{where} \quad \widetilde{\mathbf{w}} = -(\widetilde{\overline{V}})^{T} \mathbf{w}$$
 (5b)

subject to (5a) [thus assuring that all components of $\tilde{\mathbf{x}} + \tilde{\boldsymbol{\delta}}$ are positive], where $\mathbf{w} > 0$. We can nominally take the

⁵Ideally, this includes all of the strings, or at least all of the strings which we are concerned about either going slack or breaking, upon analysis of the structure under the anticipated loading conditions. The number of strings \widetilde{m} in $\widetilde{\mathbf{x}}$ must be at least as large as the number of columns of \overline{V} for the method described to be solvable.

weighting vector $\mathbf{w} = \mathbf{1}$; it may be useful⁶, however, to increase the weights somewhat on those measurable strings that, before the update (that is, as indicated in $\tilde{\mathbf{x}}$), are closest to breaking.

The problem formulated in (5a)-(5b) is easily rewritten and solved⁷ as a standard linear program (LP),

$$\overline{\mathbf{c}} = \underset{\overline{\mathbf{c}}}{\operatorname{argmax}} \overline{\mathbf{w}}^T \overline{\mathbf{c}} \quad \text{subject to} \quad \overline{A} \overline{\mathbf{c}} \le \overline{\mathbf{b}} \quad \text{and} \quad \overline{\mathbf{c}} \ge 0,$$
 (6a)

simply by decomposing $\mathbf{c} = \mathbf{c}^+ - \mathbf{c}^-$ where $\mathbf{c}^+ \geq 0$ and $\mathbf{c}^- \geq 0$, and defining $\overline{\mathbf{w}}$, $\overline{\mathbf{c}}$, \overline{A} , and $\overline{\mathbf{b}}$ as follows:

$$\overline{\mathbf{w}} = \begin{bmatrix} \widetilde{\mathbf{w}} \\ -\widetilde{\mathbf{w}} \end{bmatrix}, \quad \overline{\mathbf{c}} = \begin{bmatrix} \mathbf{c}^+ \\ \mathbf{c}^- \end{bmatrix}, \quad \overline{A} = \begin{bmatrix} -\widetilde{V} & \widetilde{V} \end{bmatrix}, \quad \overline{\mathbf{b}} = \widetilde{\mathbf{x}} - \tau_{\min} \mathbf{1}.$$
 (6b)

At any timestep in the application of this approach, once the LP in (6) is solved⁸ for $\bar{\mathbf{c}}$, the tensions in the tensionable strings (a subset of the measurable strings with winches at one end) are reset to their corresponding updated values, as evident in the corresponding element of $\mathbf{x} + \boldsymbol{\delta} = \mathbf{x} + \overline{V}\mathbf{c}$, and (assuming nonstretchable strings) the rest of the tensions in the structure will, essentially immediately (as all bars have some inertia), respond accordingly to maintain the structure at static equilibrium, while including the specified components \mathbf{c} of the nullspace vectors (the columns of \overline{V}) into the new force distribution $\mathbf{x}_{\text{new}} = \mathbf{x} + \overline{V}\mathbf{c}$ such that the minimum tensions in the measurable strings is τ_{min} , while simultaneously minimizing a weighted one-norm of the measurable string tensions, as specified in (5b).

Relaxing the idealization of nonstretchable strings, but adding the assumption that the external forcing $\mathbf{u}(t)$ varies only slowly in time as compared with the time constants of the modes of vibration of the resulting pretensioned structure, the updates to the tensions in the strings computed via this approach at each timestep may simply be passed through a suitable low-pass filter, in order to minimize the excitation of any structural vibration modes following this tensioning approach. If the external forcing $\mathbf{u}(t)$ varies too quickly for such an approach to be effective, a control approach based on a full analysis of the dynamics of the tensegrity structure (see §3) must be used instead, which involves significantly more finesse in the formulation and solution of the control problem at hand.

2.7 Static tensioning of an (underdetermined) tensegrity structure that is tensionable under load

The tensegrity structures that motivated the present work are not pretensionable; however, once the nominal load (that is, the buoyancy of the balloon and the weight of the payload, assuming the former is larger than the latter) is applied, if $\hat{r} < b + s$, there will be one or more degrees of freedom in the set of realizable solutions (with all strings in tension). These extra degrees of freedom may be set following the simple LP-based approach described in §2.6. However, it is useful to modify this approach slightly for this special case of tensegrity structures, that are said to be only tensionable under load. In such systems, only so much tension may be applied in any given string before one of the other stings goes slack (note that this is not the case in pretensionable structures); the primary concern in such systems is thus not really breaking a string, but in fact simply keeping all of the strings under tension as disturbances are applied.

It is thus desireable in this setting to change the objective in the LP discussed in §2.6 to the maximization of τ_{\min} itself, thereby in a certain respect maximizing the "margin" of additional disturbances that the structure can endure before one of the strings goes slack. Noting that the LP discussed previously is linear in τ_{\min} , this can be accomplished in the setting of (6a) simply by redefining $\overline{\mathbf{w}}$, $\overline{\mathbf{c}}$, \overline{A} , and $\overline{\mathbf{b}}$ as follows:

$$\overline{\mathbf{w}} = \begin{bmatrix} 0 \\ 0 \\ 1 \end{bmatrix}, \quad \overline{\mathbf{c}} = \begin{bmatrix} \mathbf{c}^+ \\ \mathbf{c}^- \\ \tau_{\min} \end{bmatrix}, \quad \overline{A} = \begin{bmatrix} -\widetilde{V} & \widetilde{V} & \mathbf{1} \end{bmatrix}, \quad \overline{\mathbf{b}} = \widetilde{\mathbf{x}}.$$
 (6c)

⁶Other ways of posing the problem of not allowing any of the (measurable) string tensions in $\tilde{\mathbf{x}}$ to get too large are possible. For example, if a single string material and diameter (and, thus, strength) is used everywhere, it might be preferred to minimize the infinity norm of $\tilde{\mathbf{x}}$. Formally, it is sometimes said that, in low dimensions, all norms are "equivalent", meaning in this case that the one norm bounds the infinity norm from both below and above, and vice-versa, i.e., $\|\tilde{\mathbf{x}}\|_1/\tilde{m} \leq \|\tilde{\mathbf{x}}\|_1 \leq \tilde{m} \|\tilde{\mathbf{x}}\|_{\infty}$; note, however, that these bounds become increasingly loose as the dimension \tilde{m} of the vector $\tilde{\mathbf{x}}$ is increased. Adjusting the weights in the weighted one-norm used here shifts the emphasis in the minimization problem (5b) to those directions that matter most, thus providing a solution using the one-norm that is in a sense closer to that provided using the infinity norm, while retaining the convenient structure of an LP.

⁷There are dozens of algorithms and efficient software libraries available to solve LPs, including linprog in Matlab and PuLP in Python. ⁸Note that this can be done remarkably quickly, even for relatively large \widetilde{m} , and even on a quite modest single-board computer.

2.8 Open and closed kinematic chains

The analysis of the static equilibrium of a tensegrity structure lumps all forces (including those from the weight or buoyancy of the bars) at the nodes, and effectively treats the bars and strings in the same manner, the only significant difference being that strings are not allowed to provide compressive force. Indeed, which members of a tensegrity structure are bars, and which are stings, does not actually need to be decided upon until after the initial static equilibrium analysis is complete. In many tensionable tensegrity systems, in fact, all bars can be replaced by strings, and strings by bars, and a different tensioning solution again results in a realizable tensegrity structure.

In particular, the analysis of the static equilibrium of tensegrity structures is not complicated by cases in which bars directly attach to other bars, and/or to fixed points. This is in contrast with the analysis of the *dynamics* of tensegrity structures, in which Newton's laws for the time evolution of the position and orientation of the bars are solved, with the strings that interconnect the bars simply providing forces at the nodal points on the bars to which these strings attach, in the directions of the strings themselves and with magnitude proportional to the amount that these strings are stretched from their rest length. In such a setting, *constraints* on the time evolution of the position and orientation of the bars need to be applied if bars are initially attached to fixed nodes, in order to keep them so attached, and/or if bars are initially connected to other bars (a structure called a *kinematic chain*), in order to keep them so connected; such constraints on a time evolution can substantially complicate a numerical simulation code.

In the case of *open* kinematic chains (like robot manipulator arms), there are no closed loops; that is, at least one end of any chain of connected bars in the structure terminates with a free node. In this situation, a simple change of variables suffices to recast the constrained evolution of the position and orientation of the bars into an unconstrained time evolution in the modified variables. For example, imagine a kinematic chain that begins at a fixed node and ends at a free node. The bar that is connected to the fixed node is described by its (fixed) length together with a direction vector from the fixed node, the second bar in the chain is described by its length together with a direction vector from the end of the first bar, etc.; once Newton's laws for the time evolution of such a system are recast into these modified configuration variables, the (otherwise, difficult) constraints reflecting the connectivity of the kinematic chain(s) are then simply implicit to the configuration representation itself.

In the case of closed kinematic chains (like 4-bar linkages), however, the constraints inherent to the connections in the chain can not be eliminated with a simple change of variables; this case is generally much more difficult to simulate accurately. One approach to such a problem is to put a stretchable "fictitious string" of zero nominal length from the last node of the chain back to the fixed node (or, back to one of the previous free nodes in the chain) to which it connects. The stiffer this (critically damped) fictitious string is made, the more accurately the kinematic chain will be closed. Treating (via iteration at each timestep) the effect of the force caused by this fictitious string in the expression of Newton's equations for the time evolution of this system (in this constrained setting, a descriptor system) with the L-stable implicit part of an implicit/explicit (IMEX) time marching strategy for stiff systems [5] then allows the stiffness of the (critically damped) fictitious string to be taken as large (essentially infinite) without substantially limiting the timestep required for numerical stability of the simulation.

To simplify the discussion of tensegrity dynamics in §3, we will restrict our attention to the unconstrained setting in which no bars are attached to other bars, or to fixed points, as this simplified setting (once extended to account for embedded solid bodies) is entirely sufficient for the dynamic simulation of the structures proposed in [1].

3 Dynamics of tensegrity systems with embedded solid bodies

Leveraging the precise notation defined in $\S2$, and noting in particular the discussion of open and closed kinematic chains in $\S2.8$, we now succinctly review the dynamics of 3D (i.e., d=3) unconstrained class 1 tensegrity systems with *embedded solid bodies*, generalizing the analysis presented in chapter 5 of [10], assuming that:

(a) each string is massless, exhibiting linear elastic behaviour when in tension and zero force when slack, such that each element of the vector $\mathbf{x}^{\mathbf{s}}$ of tension forces in the strings is now given by

$$x_j^{s} = \max\{0, \kappa_j(\|\vec{s}_j\| - \ell_j^{s,0})/\ell_j^{s,0})\},$$
 (7)

where $\ell_i^{\,\mathrm{s},0}$ denotes the rest length of string \vec{s}_j (for the tether material considered in [1], $\kappa \approx 60/0.02 = 3000$),

- (b) each bar is rigid and slender, so that the degree of freedom (DOF) corresponding to rotation of each bar about its long axis may be neglected, with strings attached to the free nodes at each end,
- (c) each solid body has three nonzero principal moments of inertia $J_1 \ge J_2 \ge J_3 > 0$, so all three rotational DOF may be significant, with one or more free nodes affixed to the body at which strings may be attached,
- (d) the tensegrity system is, in the language of [10], unconstrained class 1, meaning that each bar (and, each embedded solid body) is only attached to strings (that is, not to other bars, nor to other solid bodies) and that the nodal points

on each bar and on each solid body are free (not fixed), and

(e) the connectivity of the members (strings, bars, and solid bodies) between the nodes (free and fixed) in the structure is prescribed by the connectivity matrix C, as denoted and defined in (2), with the columns of C^T corresponding to each solid body containing entries equal to 1 for each node (i.e., at each string attachment point) on the solid body.

Given these assumptions, the dynamics of the entire tensegrity structure is then described simply by writing Newton's laws for the time evolution of the linear and angular momentum of the bars and solid bodies, with the strings applying forces to the free nodes (at the ends of the bars, and at the attachment points on the solid bodies) at any instant as specified by (7). Rather than applying the conditions of static equilibrium, as done in §2 [see (4)], the (not necessarily balanced) forces at the nodes due to the tension and compression of the members, together with the external forces \mathbf{u} (including both disturbance forces as well as the weight or buoyancy of the bars and solid bodies) and reaction forces \mathbf{v} , apply net forces and torques which affect this time evolution, generally resulting, due to the elasticity of the strings, in both net deflections and possibly significant vibrations of the structure under time-varying loads. [Note that many tensegrity structures are only lightly damped before feedback control is applied.]

3.1 Notation used for dynamic model of tensegrity system

To proceed, define the bar location \vec{r}_k^b as the vector in \mathbb{R}^3 from the origin to the center of mass of bar b_k , the two ends nodes of which are denoted $\vec{n}_{k,1}^b$ and $\vec{n}_{k,2}^b$ (i.e., $\vec{b}_k = \vec{n}_{k,1}^b - \vec{n}_{k,2}^b$). Recall the definition of the bar length $\ell_k^b = \|\vec{b}_k\|$ and the (normalized) bar direction $\vec{d}_k^b = \vec{b}_k/\ell_k^b$ which, noting assumption (b) above, uniquely defines the orientation of the bar. To simplify the discussion that follows, we also assume that the mass distribution of each bar is uniform, so that $\vec{r}_k^b = (\vec{n}_{k,1}^b + \vec{n}_{k,2}^b)/2$, and

$$\vec{n}_{k,1}^{\,b} = \vec{r}_k^{\,b} + (\ell_k^{\,b}/2)\,\vec{d}_k^{\,b}, \qquad \vec{n}_{k,2}^{\,b} = \vec{r}_k^{\,b} - (\ell_k^{\,b}/2)\,\vec{d}_k^{\,b}.$$
 (8a)

[Note that this simplification is easily relaxed.] With these assumptions, the moment of inertia J_k^b of a (slender, uniform) bar \vec{b}_k with mass m_k , when rotated about its own center of mass and about an axis perpendicular to the bar direction vector \vec{d}_k^b , is $J_k^b = m_k \ell_k^2/12$. The ODEs governing the 5 DOF dynamics of a bar (that is, the time evolution of $\{\vec{r}_k^b, \vec{d}_k^b\}$ subject to $\|\vec{d}_k^b\| = 1$) is laid out in §3.2.

Define also the solid body location \vec{r}_k^{σ} as the vector in \mathbb{R}^3 from the origin to the center of mass of solid body σ_k with principal moments $J_{k,1}^{\sigma} \geq J_{k,2}^{\sigma} \geq J_{k,3}^{\sigma} > 0$, the a_k attachment nodes on which are defined in the (unrotated) principal coordinates of the body as $\vec{n}_{k,1}^{\sigma,B}, \ldots, \vec{n}_{k,a_k}^{\sigma,B}$, and are denoted in global coordinates as $\vec{n}_{k,1}^{\sigma}, \ldots, \vec{n}_{k,a_k}^{\sigma}$. The configuration of the solid body in the global frame is defined as a rotation and translation from a nominal configuration in the body frame B, in which the center of mass of the body is at the origin and the principal axes of the body are aligned with the $\{x,y,z\}$ axes, via a corresponding (4-component) unit quaternion \mathbf{d}_k^{σ} (reviewed in §3.3) such that

$$\vec{n}_{k,i}^{\sigma} = \vec{r}_k^{\sigma} + \mathbf{d}_k^{\sigma} \, \vec{n}_{k,i}^{\sigma,B} \left(\mathbf{d}_k^{\sigma} \right)^* \quad \text{for } i = 1, \dots, a_k.$$
(8b)

The ODEs governing the 6 DOF dynamics of a solid body (that is, the time evolution of $\{\vec{r}_k^{\sigma}, \mathbf{d}_k^{\sigma}\}$ subject to $\|\mathbf{d}_k^{\sigma}\| = 1$) is laid out in §3.3.

The dynamics of an entire unconstrained class 1 tensegrity system with embedded solid bodies is then given simply by interconnecting its b bars (see §3.2), σ solid bodies (see §3.3), and p fixed nodes with s elastic strings, the tension of which is governed by (7), as summarized in §3.4.

3.2 5 DOF dynamics of $\{\vec{r}, \vec{d}\}$ of a single bar, with unit vector \vec{d} defining bar direction

For notational convenience in this subsection only, which focuses exclusively on bar b_k , we drop the k subscript and b superscript on all variables. Given this, the linear momentum of the bar is simply $(m \, \dot{\vec{r}})$, and its angular momentum \vec{h} may be written as the product of the moment of inertia of the bar about its center, J, and the cross product of the normalized bar direction vector \vec{d} with its time derivative $\dot{\vec{d}}$, noting that $\|\vec{d}(t)\| = 1$ for all t:

$$\vec{h} = J \, \vec{d} \times \dot{\vec{d}} = J \, \widetilde{D} \, \dot{\vec{d}} \quad \text{where} \quad \widetilde{D} = \begin{pmatrix} 0 & -d_3 & d_2 \\ d_3 & 0 & -d_1 \\ -d_2 & d_1 & 0 \end{pmatrix}. \tag{9}$$

We are now in a position to write Newton's laws for the time evolution of the linear and angular momentum of the bar. The linear acceleration of the bar is, of course, governed simply by

$$m\ddot{\vec{r}} = \vec{f_1} + \vec{f_2} + \vec{u} \tag{10}$$

where $\vec{f_1}$ is the sum of all string forces at one end of the bar, $\vec{f_2}$ is the sum of all string forces at the other end of the bar, and \vec{u} includes all additional forces on the bar. Similarly, differentiating (9) and noting that $\vec{a} \times \vec{a} = 0$ for any vector \vec{a} , the angular acceleration of the bar is governed by

$$d\vec{h}/dt = \dot{\vec{h}} = J \ \vec{d} \times \ddot{\vec{d}} = J \ \widetilde{\vec{D}} \ \ddot{\vec{d}} = \vec{\tau} = \vec{d} \times \vec{\phi} = \widetilde{\vec{D}} \ \vec{\phi} \quad \text{where} \quad \vec{\phi} = \eta_1 \ \vec{f}_1 + \eta_2 \ \vec{f}_2 + \eta_3 \ \vec{u}, \tag{11}$$

where $\vec{\phi}$ (the generalized force driving the evolution equation for \vec{d}) is such that $\vec{\tau} = \vec{d} \times \vec{\phi}$, and thus $\vec{\phi}$ arises due to the forces applied at its ends, $\vec{f_1}$ and $\vec{f_2}$, acting via moment arms of $\eta_1 = \ell/2$ and $\eta_2 = -\ell/2$ respectively, as well as the sum of all additional forces acting on the bar, \vec{u} , acting via some cumulative third moment arm η_3 , the modeling of which is problem specific (often, $\eta_3 = 0$). We now apply the constraint that $||\vec{d}|| = 1$, and thus, via differentiation,

$$\|\vec{d}\|^2 = \vec{d}^T \vec{d} = 1 \quad \Rightarrow \quad \vec{d}^T \dot{\vec{d}} = 0 \quad \Rightarrow \quad \vec{d}^T \ddot{\vec{d}} + \|\dot{\vec{d}}\|^2 = 0.$$
 (12)

Note that \widetilde{D} is singular (in particular, $\widetilde{D} \vec{d} = 0$), and thus (11) alone is insufficient to define the evolution of \vec{d} . Thus, writing $J \widetilde{D} \ddot{\vec{d}} = \vec{\tau}$ from (11) and $\vec{d}^T \ddot{\vec{d}} + \|\dot{\vec{d}}\|^2 = 0$ from (12) as a system of simultaneous equations gives

$$A_1 \ddot{\vec{d}} = \begin{bmatrix} \vec{\tau}/J \\ -\|\dot{\vec{d}}\|^2 \end{bmatrix} \quad \text{where} \quad A_1 = \begin{bmatrix} \tilde{D} \\ \vec{d}^T \end{bmatrix}. \tag{13}$$

This system of simultaneous equations may be simplified (again, following [10]) by first noting that

$$A_{1}^{T} A_{1} = \begin{bmatrix} \widetilde{D}^{T} & \vec{d} \end{bmatrix} \begin{bmatrix} \widetilde{D} \\ \vec{d}^{T} \end{bmatrix} = \begin{pmatrix} 0 & d_{3} & -d_{2} & d_{1} \\ -d_{3} & 0 & d_{1} & d_{2} \\ d_{2} & -d_{1} & 0 & d_{3} \end{pmatrix} \begin{pmatrix} 0 & -d_{3} & d_{2} \\ d_{3} & 0 & -d_{1} \\ -d_{2} & d_{1} & 0 \\ d_{1} & d_{2} & d_{3} \end{pmatrix} = \begin{pmatrix} \|\vec{d}\|^{2} & 0 & 0 \\ 0 & \|\vec{d}\|^{2} & 0 \\ 0 & 0 & \|\vec{d}\|^{2} \end{pmatrix} = \|\vec{d}\|^{2} I$$

$$\Rightarrow \widetilde{D}^{T} \widetilde{D} + \vec{d} \vec{d}^{T} = \|\vec{d}\|^{2} I. \tag{14a}$$

The columns of A_1 are seen to be orthogonal, each with norm $\|\vec{d}\|^2$. The matrix

$$A_1^+ = A_1^T / \|\vec{d}\|^2 = \left[\tilde{D}^T \quad \vec{d} \right] / \|\vec{d}\|^2$$
 (14b)

is thus the (unique) left inverse of the (full-rank) 4×3 matrix A_1 , and the unique solution of (13), noting (14), is

$$\vec{d} = A_1^+ \begin{bmatrix} \vec{\tau}/J \\ -\|\vec{d}\|^2 \end{bmatrix} = \begin{bmatrix} \widetilde{D}^T & \vec{d} \end{bmatrix} \begin{bmatrix} \vec{\tau}/J \\ -\|\vec{d}\|^2 \end{bmatrix} / \|\vec{d}\|^2 = \widetilde{D}^T \widetilde{D} \vec{\phi} / (J \|\vec{d}\|^2) - \vec{d} \|\vec{d}\|^2 / \|\vec{d}\|^2
\Rightarrow \qquad \ddot{\vec{d}} = \{I - \vec{d} \vec{d}^T / \|\vec{d}\|^2\} (\eta_1 \vec{f}_1 + \eta_2 \vec{f}_2 + \eta_3 \vec{u}) / J - (\|\vec{d}\|/\|\vec{d}\|)^2 \vec{d}. \tag{15}$$

As an (equivalent) alternative to the second-order ODE in (15), one can instead march a pair of first-order ODEs when simulating the time evolution of the bar direction \vec{d} by writing $\widetilde{D} \, \dot{\vec{d}} = \vec{h}/J$ from (9) and $\vec{d}^T \dot{\vec{d}} = 0$ from (12) as a system of simultaneous equations, leveraging (14b) as before, and noting (11), thus giving

$$A_1 \dot{\vec{d}} = \begin{bmatrix} \vec{h}/J \\ 0 \end{bmatrix} \quad \Rightarrow \quad \dot{\vec{d}} = \begin{bmatrix} \widetilde{D}^T & \vec{d} \end{bmatrix} \begin{bmatrix} \vec{h}/J \\ 0 \end{bmatrix} / \|\vec{d}\|^2 \quad \Rightarrow \quad \dot{\vec{d}} = \widetilde{D}^T \vec{h}/(J\|\vec{d}\|^2), \quad \dot{\vec{h}} = \widetilde{D} \left(\eta_1 \vec{f}_1 + \eta_2 \vec{f}_2 + \eta_3 \vec{u} \right). \quad (16)$$

Equations (10) and (15) [alternatively, the pair of first-order forms in (16)] thus give the ODEs governing the time evolution of the 5 DOF defining the configuration of the bar in 3D, as defined by $\{\vec{r}, \vec{d}\}$ and influenced by $\{\vec{f_1}, \vec{f_2}, \vec{u}\}$, which includes the forces due to the tensions of the strings attached to its two ends, $\vec{f_1}$ and $\vec{f_2}$, as well as \vec{u} , which includes all additional forces on the bar (due to external disturbances and the weight or buoyancy of the bar itself). Note that this system evolves on the manifold $||\vec{d}|| = 1$, which is enforced in (15) by incorporating $\vec{d}^T \vec{d} + ||\vec{d}||^2 = 0$ from (12), and is enforced in (16) by incorporating $\vec{d}^T \vec{d} = 0$ from (12). Time marching errors can lead to $||\vec{d}||$ drifting away from unity during the numerical simulation of either form; occasionally renormalizing \vec{d} during such a simulation can easily correct for such errors. For further discussion and comparison of the numerical stability of these forms, see [6].

3.3 6 DOF dynamics of $\{\vec{r}, d\}$ of a single solid body, with unit quaternion d defining body orientation

For notational convenience in this subsection only, which focuses exclusively on solid body σ_k , we drop the k subscript and σ superscript on all variables. As before, the linear acceleration of the solid body is governed simply by

$$m \, \ddot{\vec{r}} = \sum_{i=1}^{a} \vec{f_i} + \vec{u} \tag{17}$$

where $\vec{f_i}$ is the force is due to all of the strings connected at each of the a attachment points on the solid body, and \vec{u} includes all additional forces on the solid body.

We now review the framework for the rotational dynamics of solid bodies leveraging quaternions⁹. The *unit* quaternion $\mathbf{d} = d_0 + d_1 \mathbf{i} + d_2 \mathbf{j} + d_3 \mathbf{k}$ is taken to represent the rotation of any vector \vec{p}^B in the <u>B</u>ody frame (e.g., to any specific point \vec{p}^B on the solid body) to the corresponding vector \vec{p} in the global frame, giving¹⁰

$$\vec{p} = \mathbf{d} \, \vec{p}^B \mathbf{d}^* = \begin{pmatrix} (d_0^2 + d_1^2 - d_2^2 - d_3^2) & 2(d_1 d_2 - d_0 d_3). & 2(d_1 d_3 + d_0 d_2) \\ 2(d_1 d_2 + d_0 d_3) & (d_0^2 - d_1^2 + d_2^2 - d_3^2) & 2(d_2 d_3 - d_0 d_1) \\ 2(d_1 d_3 - d_0 d_2) & 2(d_2 d_3 + d_0 d_1). & (d_0^2 - d_1^2 - d_2^2 + d_3^2) \end{pmatrix} \vec{p}^B,$$
(19)

where $\mathbf{d}^* = d_0 - d_1 \mathbf{i} - d_2 \mathbf{j} - d_3 \mathbf{k}$ denotes the conjugate of unit quaternion \mathbf{d} , with $\|\mathbf{d}\|^2 = \mathbf{d}^* \mathbf{d} = \mathbf{d} \mathbf{d}^* = d_0^2 + d_1^2 + d_2^2 + d_3^2 = 1$. Leveraging the constraint $\|\mathbf{d}\|^2 = 1$, it may be shown that

$$\dot{\mathbf{d}} = \vec{\omega} \, \mathbf{d}/2 = \mathbf{d} \, \vec{\omega}^B / 2 \tag{20}$$

where $\vec{\omega}^B$ is the *instantaneous rate of rotation* of the body in the body frame, and $\vec{\omega}$ is the corresponding representation of this instantanous rate of rotation in the global frame. It may also be shown that, in the body frame (rotating with the solid body, with inertial matrix J), Euler's equations of motion are

$$J\dot{\vec{\omega}}^B + \vec{\omega}^B \times (J\vec{\omega}^B) = \vec{\tau}^B, \tag{21a}$$

where $\vec{\tau}^B$ is the total torque applied to the body about each of its (body-fixed) coordinate axes; if these coordinate axes are aligned with the principal coordinate directions of the body, Euler's equations (21a) conveniently reduce to

$$J_1 \dot{\omega}_1^B + (J_3 - J_2) \omega_2^B \omega_3^B = \tau_1^B, \quad J_2 \dot{\omega}_2^B + (J_1 - J_3) \omega_3^B \omega_1^B = \tau_2^B, \quad J_3 \dot{\omega}_3^B + (J_2 - J_1) \omega_1^B \omega_2^B = \tau_3^B. \tag{21b}$$

The torque $\vec{\tau}^B$, in turn, is related to the forces \vec{f}_i due to all of the strings connected at each of the $i=1,\ldots,a$ attachment points, as well as the additional forces on the solid body \vec{u} , as follows

$$\vec{\tau}^B = \sum_{i=1}^a \vec{n}_i^B \times \vec{f}_i^B + \vec{\eta}^B \times \vec{u}^B \quad \text{where} \quad \vec{f}_i^B = \mathbf{d}^* \vec{f}_i \mathbf{d}, \quad \vec{u}^B = \mathbf{d}^* \vec{u} \mathbf{d}$$
 (22a)

where, as mentioned previously, the a attachment nodes on the body are defined in the principal coordinates of the body as $\vec{n}_1^B, \dots, \vec{n}_a^B$, and the modeling of moment arm $\vec{\eta}^B$ is problem specific (often, $\vec{\eta}^B = 0$). Taking the time derivative of $\dot{\mathbf{d}} = \mathbf{d} \vec{\omega}^B/2$ from (20) and substituting (21a) and $\vec{\omega}^B = 2 \mathbf{d}^* \dot{\mathbf{d}}$ results in a nonlinear second-order equation for the time evolution of the unit quaternion \mathbf{d} :

$$\ddot{\mathbf{d}} = \left\{ \dot{\mathbf{d}} \,\vec{\omega}^B + \mathbf{d} \,\dot{\vec{\omega}}^B \right\} / 2 = \left\{ \dot{\mathbf{d}} \,\vec{\omega}^B + \mathbf{d} J^{-1} [\vec{\tau}^B - \vec{\omega}^B \times (J \,\vec{\omega}^B)] \right\} / 2$$

$$\Rightarrow \quad \ddot{\mathbf{d}} = \dot{\mathbf{d}} \,\mathbf{d}^* \,\dot{\mathbf{d}} + \mathbf{d} J^{-1} [\vec{\tau}^B - 4 \,\mathbf{d}^* \dot{\mathbf{d}} \times (J \,\mathbf{d}^* \dot{\mathbf{d}})] / 2. \tag{22b}$$

$$\mathbf{i}^2 = \mathbf{j}^2 = \mathbf{k}^2 = \mathbf{i}\mathbf{j}\mathbf{k} = -1 \quad \Rightarrow \quad \mathbf{i}\mathbf{j} = -\mathbf{j}\mathbf{i} = \mathbf{k}, \quad \mathbf{j}\mathbf{k} = -\mathbf{k}\mathbf{j} = \mathbf{i}, \quad \mathbf{k}\mathbf{i} = -\mathbf{i}\mathbf{k} = \mathbf{j}, \tag{18a}$$

the Hamilton product of two quaternions $\mathbf{p} = p_0 + p_1 \mathbf{i} + p_2 \mathbf{j} + p_3 \mathbf{k} = p_0 + \vec{p}$ and $\mathbf{q} = q_0 + q_1 \mathbf{i} + q_2 \mathbf{j} + q_3 \mathbf{k} = q_0 + \vec{q}$, where $\vec{p} = p_1 \mathbf{i} + p_2 \mathbf{j} + p_3 \mathbf{k}$ and $\vec{q} = q_1 \mathbf{i} + q_2 \mathbf{j} + q_3 \mathbf{k}$, treats \mathbf{i} , \mathbf{j} , and \mathbf{k} like noncommutative algebraic variables; applying (18a), this results in

$$\mathbf{r} = \mathbf{p}\,\mathbf{q} = r_0 + r_1\mathbf{i} + r_2\mathbf{j} + r_3\mathbf{k} = (p_0 + \vec{p})(q_0 + \vec{q}) = (p_0q_0 - \vec{p} \cdot \vec{q}) + (p_0\vec{q} + q_0\vec{p} + \vec{p} \times \vec{q})$$
(18b)

$$\Rightarrow \begin{pmatrix} r_0 \\ r_1 \\ r_2 \\ r_3 \end{pmatrix} = \begin{pmatrix} p_0 & -p_1 & -p_2 & -p_3 \\ p_1 & p_0 & -p_3 & p_2 \\ p_2 & p_3 & p_0 & -p_1 \\ p_3 & -p_2 & p_1 & p_0 \end{pmatrix} \begin{pmatrix} q_0 \\ q_1 \\ q_2 \\ q_3 \end{pmatrix} = \begin{pmatrix} q_0 & -q_1 & -q_2 & -q_3 \\ q_1 & q_0 & q_3 & -q_2 \\ q_2 & -q_3 & q_0 & q_1 \\ q_3 & q_2 & -q_1 & q_0 \end{pmatrix} \begin{pmatrix} p_0 \\ p_1 \\ p_2 \\ p_3 \end{pmatrix}, \tag{18c}$$

where $\vec{p} \cdot \vec{q}$ and $\vec{p} \times \vec{q}$ denote 3D dot and cross products. Equations like (19) treat vectors in \mathbb{R}^3 like quaternions with zero real part.

¹⁰Writing $\mathbf{d} = e^{\vec{u} \phi} = e^{(u_1 \mathbf{i} + u_2 \mathbf{j} + u_3 \mathbf{k}) \phi} = \cos \phi + (u_1 \mathbf{i} + u_2 \mathbf{j} + u_3 \mathbf{k}) \sin \phi$ for $||\vec{u}|| = 1$, (19) gives a clockwise rotation of \vec{p}^B about the unit vector \vec{u} by an angle $\theta = 2\phi$.

⁹Based on Hamilton's 1843 construction

Note also the constraint that $\|\mathbf{d}\| = 1$, and thus, via differentiation,

$$\|\mathbf{d}\|^2 = \mathbf{d}^*\mathbf{d} = 1 \quad \Rightarrow \quad \mathbf{d}^*\dot{\mathbf{d}} + \dot{\mathbf{d}}^*\mathbf{d} = 2[\mathbf{d}^*\dot{\mathbf{d}}]_0 = 0 \quad \Rightarrow \quad \mathbf{d}^*\ddot{\mathbf{d}} + \ddot{\mathbf{d}}^*\mathbf{d} + 2\dot{\mathbf{d}}^*\dot{\mathbf{d}} = 0 \quad \Rightarrow \quad [\mathbf{d}^*\ddot{\mathbf{d}}]_0 = -\dot{\mathbf{d}}^*\dot{\mathbf{d}}, \tag{23}$$

where $[\mathbf{p}]_0$ denotes the real part of \mathbf{p} . Note that (22b) is consistent with this constraint, which is used implicitly in the writing of (20) upon which it is derived. This may be seen by defining $\mathbf{p} = \mathbf{d}^*\dot{\mathbf{d}}$ (note that, by (23), $[\mathbf{p}]_0 = 0$, and thus \mathbf{p} may, by footnote 9, be denoted by its vector part \vec{p}) and premultiplying (22b) by \mathbf{d}^* , leading to

$$\mathbf{d}^*\ddot{\mathbf{d}} = \mathbf{p}\,\mathbf{p} + \|\mathbf{d}\|^2 J^{-1}[\vec{\tau}^B - 4\,\vec{p} \times (J\,\vec{p})]/2;$$

by (18b), the first term on the RHS is the real part of $\mathbf{d}^*\ddot{\mathbf{d}}$, and the second term is the vector part of $\mathbf{d}^*\ddot{\mathbf{d}}$. Note in particular that this formula gives $[\mathbf{d}^*\ddot{\mathbf{d}}]_0 = \mathbf{p}\,\mathbf{p} = -\mathbf{p}^*\mathbf{p} = -\dot{\mathbf{d}}^*\mathbf{d}\,\mathbf{d}^*\dot{\mathbf{d}} = -\dot{\mathbf{d}}^*\dot{\mathbf{d}}$, as required by (23).

As an (equivalent) alternative to the second-order ODE in (22a)-(22b), one can instead march a pair of first-order ODEs when simulating the time evolution of the solid body orientation \mathbf{d} via $\dot{\mathbf{d}} = \mathbf{d} \vec{\omega}^B/2$ from (20), which is inherently consistent with $[\mathbf{d}^*\dot{\mathbf{d}}]_0 = 0$ from (23), in parallel with (21a) [or (21b), as appropriate].

Noting (22a), equations (17) and (22b) [alternatively, the pair of first-order forms (20) and (21a) or (21b)] thus give the ODEs governing the time evolution of the 6 DOF defining the configuration of the solid body in 3D, as defined by $\{\vec{r}, \mathbf{d}\}$ and influenced by $\{\vec{f}_1, \dots, \vec{f}_a, \vec{u}\}$, which includes the forces due to the tensions of the strings attached to each of its a attachments points, \vec{f}_1 to \vec{f}_a , as well as \vec{u} , which includes all additional forces on the solid body (due to external disturbances and the weight or buoyancy of the solid body itself). Note that this system evolves on the manifold $\|\mathbf{d}\| = 1$. Again, time marching errors can lead to $\|\mathbf{d}\|$ drifting away from unity during the numerical simulation of either form; occasionally renormalizing \mathbf{d} during such a simulation can correct for such errors. For further discussion, see [8, 9].

3.4 Dynamics of an entire tensegrity structure

The complete set of equations governing the dynamics [that is, the time evolution of the configuration vector $\mathbf{q}(t)$] of an entire elastic class 1 tensegrity system, with bars and solid bodies interconnected by elastic strings, in response to (nominal plus disturbance) time-varying loads $\mathbf{u}(t)$, may now be pieced together. This set of equations is given by the dynamic equations for the time evolution of the position and direction $\{\vec{r}_k^b, \vec{d}_k^b\}$ of each individual bar b_k , as given in (10) and (16) [using the pair of first-order forms for the bar direction]:

$$\ddot{\vec{r}}_k^b = (\vec{f}_{k,1}^b + \vec{f}_{k,2}^b + \vec{u}_k^b)/m_k^b, \tag{24a}$$

$$\dot{\vec{d}}_{k}^{b} = -\vec{d}_{k}^{b} \times \vec{h}_{k}^{b} / (J_{k}^{b} \| \vec{d}_{k}^{b} \|^{2}), \qquad \dot{\vec{h}}_{k}^{b} = \vec{d}_{k}^{b} \times (\eta_{k,1}^{b} \vec{f}_{k,1}^{b} + \eta_{k,2}^{b} \vec{f}_{k,2}^{b} + \eta_{k,3}^{b} \vec{u}_{k}^{b}), \tag{24b}$$

and time evolution of the position and orientation $\{\vec{r}_k^{\sigma}, \mathbf{d}_k^{\sigma}\}$ of each individual solid body σ_k , as given in (17) and (20)-(21b)-(22a) [using the pair of first-order forms, in principal coordinates, for the solid body orientation]:

$$\ddot{\vec{r}}_k^{\sigma} = \left(\sum_{i=1}^a \vec{f}_{k,i}^{\sigma} + \vec{u}_k^{\sigma}\right) / m_k^{\sigma}, \tag{24c}$$

$$\dot{\mathbf{d}}_{k}^{\sigma} = \mathbf{d}_{k}^{\sigma} \, \vec{\omega}_{k}^{\sigma,B} / 2, \qquad \dot{\vec{\omega}}_{k}^{\sigma,B} = \begin{pmatrix} [\tau_{k,1}^{\sigma,B} - (J_{k,3}^{\sigma} - J_{k,2}^{\sigma}) \, \omega_{k,2}^{\sigma,B} \, \omega_{k,3}^{\sigma,B}] / J_{k,1}^{\sigma} \\ [\tau_{k,2}^{\sigma,B} - (J_{k,1}^{\sigma} - J_{k,3}^{\sigma}) \, \omega_{k,3}^{\sigma,B} \, \omega_{k,1}^{\sigma,B}] / J_{k,2}^{\sigma} \\ [\tau_{k,3}^{\sigma,B} - (J_{k,2}^{\sigma} - J_{k,1}^{\sigma}) \, \omega_{k,1}^{\sigma,B} \, \omega_{k,2}^{\sigma,B}] / J_{k,3}^{\sigma} \end{pmatrix},$$
(24d)

where
$$\vec{\tau}_k^{\sigma,B} = \sum_{i=1}^a \vec{n}_{k,i}^{\sigma,B} \times \left[(\vec{\mathbf{d}}_k^{\sigma})^* \vec{f}_{k,i}^{\sigma} \mathbf{d}_k^{\sigma} \right] + \vec{\eta}_k^{\sigma,B} \times \left[(\mathbf{d}_k^{\sigma})^* \vec{u}_k^{\sigma} \mathbf{d}_k^{\sigma} \right].$$
 (24e)

The dynamics of the bars are influenced by the forces $\vec{f}_{k,1}^b$ and $\vec{f}_{k,2}^b$ due to the tensions of the strings attached to the end nodes on each bar, $\vec{n}_{k,1}^b$ and $\vec{n}_{k,2}^b$, and \vec{u}_k^b , which includes all additional forces on each bar, and the dynamics of the solid bodies are influenced by the forces $\vec{f}_{k,1}^\sigma$ to \vec{f}_{k,a_k}^σ due to the tensions of the strings attached to each of the a_k attachment nodes on each solid body, $\vec{n}_{k,1}^\sigma$ to \vec{n}_{k,a_k}^σ , and \vec{u}_k^σ , which includes all additional forces on each solid body. To determine the forces from the strings, the locations of the end nodes on each bar, $\vec{n}_{k,1}^b$ and $\vec{n}_{k,2}^b$, are first related to the bar positions and directions, $\{\vec{r}_k^b, \vec{d}_k^b\}$, as in (8a), and the locations of the attachment nodes on the solid bodies, $\vec{n}_{k,1}^\sigma$ to \vec{n}_{k,a_k}^σ , are related to the solid body positions and orientations, $\{\vec{r}_k^\sigma, \mathbf{d}_k^\sigma\}$, as in (8b). Defining

$$\begin{split} \mathbf{q} &= \begin{pmatrix} \vec{n}_{1,1}^b & \vec{n}_{1,2}^b & \dots & \vec{n}_{b,1}^b & \vec{n}_{b,2}^b & \vec{n}_{1,1}^\sigma & \dots & \vec{n}_{1,a_1}^\sigma & \dots & \vec{n}_{\sigma,1}^\sigma & \dots & \vec{n}_{\sigma,a_\sigma}^\sigma \end{pmatrix}, \\ \widehat{\mathbf{q}} &= \begin{pmatrix} \vec{r}_1^b & \vec{d}_1^b & \dots & \vec{r}_b^b & \vec{d}_b^b & \vec{r}_1^\sigma & \mathbf{d}_1^\sigma & \dots & \vec{r}_\sigma^\sigma & \mathbf{d}_\sigma^\sigma \end{pmatrix}, \end{split}$$

and noting the two matrix forms for quaternion multiplication in (18c), the linear relations in (8a)-(8b) may easily be written in matrix form $\mathbf{q} = \Xi \, \widehat{\mathbf{q}}$, where (in 3D) $\Xi = \Xi_{3(2b+a_a+a_2+...+a_\sigma)\times(6b+7\sigma)}$ is block diagonal. Finally, the forces due to the tensions in the strings can easily be determined from the locations of the free and fixed nodes, \mathbf{q} and \mathbf{p} , via the elasticity (stretch-to-tension) relationship (7), leveraging the connectivity relationship $S = \begin{bmatrix} Q & P \end{bmatrix} C_S^T$ defining the string vectors \vec{s}_j , the (normalized) direction of each of these strings, $\vec{d}_j^s = \vec{s}_j/\ell_j^s$, and the degree to which the length of each of these strings, $\ell_j^s = \|\vec{s}_j\|$, is stretched beyond its rest length $\ell_j^{s,0}$.

Again, time marching errors can lead to $\|\vec{d}_k^b\|$ and $\|\mathbf{d}_k^\sigma\|$ durifying away from unity during numerical simulations of these equations; occasionally renormalizing \vec{d}_k^b and \mathbf{d}_k^σ during such simulations can easily correct for such errors. Note also that the vector of (nominal plus disturbance) forces \mathbf{u} acting on the system in this dynamic formulation is, perhaps most naturally, modelled for each bar and solid body, not for each node [cf. the definition of \mathbf{u} in §2].

4 Conclusions

The statics of unconstrained class-1 tensegrity structures with embedded solid bodies was first considered (in §2), extending the standard framework established by [10] to discuss not only

- (a) an effective technique (leveraging a simple LP) to optimize the static tensioning of tensegrity systems that are pretensionable, by minimizing a weighted one norm of the tensions in the strings (thus reducing the maximum tension in the tethers, thereby reducing the forces that must be applied by the winches and reducing the likelihood of a tether from breaking) while keeping the minimum tension in all strings greater than some specified τ_{\min} (thus minimizing the possibility of one of the strings going slack and fouling), while holding the embedded solid bodies in the desired pose, but also
- (b) an effective technique (leveraging a slightly modified LP) to optimize the tensioning of tensegrity systems that are only tensionable under load, such as a multiply-tethered balloon/payload system, by maximizing the minimum tension τ_{\min} of the strings (thus minimizing the possibility of one of the strings going slack and fouling) while holding the balloon/payload in the desired pose.

The general equations of motion for the dynamics of unconstrained class-1 tensegrity structures with embedded solid bodies were then derived (in §3). The formulation used is based on unit vectors \vec{d}_k^b defining the directions of the bars and, quite analogously, unit quaternions \mathbf{d}_k^{σ} defining the orientations of the solid bodies. The entire streamlined dynamics formulation avoids the calculation of trigonometric functions altogether, rendering it particularly well suited to execute quickly, in an estimation setting, on small embedded processors without dedicated hardware CORDIC subunits for the fast computation of special functions. These equations of motion are fully implemented in a new software package, TenSim (see https://github.com/tbewley/TenSim), simulations of which (as specifically applied to practical rigging designs for multiply-tethered 3D balloon/payload systems with applied external disturbances) will be reported in a follow-on paper [1].

Acknowledgements

The author very gratefully acknowledges numerous inspirations from the work of Prof Robert Skelton, whose brilliant research and meticulous teaching in tensegrity systems (see, e.g., [10]) laid the essential foundation for this study.

The author also gratefully acknowledges the financial support of JPL, Caltech, under a contract with NASA in support of this work, and would like to personally thank Fred Hadaegh, David Hanks, Adrian Stoica, S. Ryan Alimo, and Mike Pauken at JPL for their support of this effort.

References

- [1] Bewley, T (2021) Stabilization of low-altitude balloon systems, Part 2: riggings with multiple taut ground tethers, analyzed as tensegrity systems. Submitted.
- [2] Bewley, T (2021) Exponential stabilization of a variable-length pendulum with nonlinear feedback and a curious caveat. Submitted.
- [3] Bewley, T (2021) Stabilization of low-altitude balloon systems, Part 1: rigging with a single taut ground tether, analyzed as a variable-length pendulum. Submitted.
- [4] P. Miermeister et al., (2016) The CableRobot simulator large scale motion platform based on cable robot technology, *IROS*, pp. 3024-3029, doi: 10.1109/IROS.2016.7759468.

- [5] Cavaglieri, D., & Bewley, T.R. (2015) Low-storage implicit/explicit Runge-Kutta schemes for the simulation of stiff high-dimensional ODE systems, *Journal of Computational Physics* **286**, 172-193.
- [6] de Oliveira, M. (2006) Dynamics of Systems with Rods IEEE Conference on Decision & Control, 2326-2331.
- [7] Masic, M., Skelton, R.E., & Gill, P.E. (2006) Optimization of tensegrity structures. *International Journal of Solids and Structures* **43** (16), 4687-4703.
- [8] Meirovitch, L. (1970) Methods of Analytic Dynamics. McGraw-Hill.
- [9] Shabana, A.A. (2003) Dynamics of Multibody Systems. Cambridge University Press, 2nd ed..
- [10] Skelton, R.E., & de Oliveira, M.C. (2009) Tensegrity Systems. Springer.